Estimating the effects of systematic errors in *Fermi*-LAT data

S. J. Fegan[1], J. Chiang[2], E. Charles[2], P. Bruel[1] & N. Omodei[2]

on behalf of the *Fermi*-LAT collaboration

[1] Laboratoire Leprince Ringuet / Ecole Polytechnique, Palaiseau, France

[2] KIPAC, SLAC National Accelerator Lab, Stanford University, Stanford, USA

2011 Fermi Symposium, 09-12 May 2011, Rome, Italy

We discuss methods to estimate the effects of systematic errors on spectral fits to *Fermi*-LAT data.

Abstract: The Fermi LAT detects cosmic gamma-rays in the E>20MeV energy regime. The Fermi science tools allow users to fit the LAT data with a model for the spatial and spectral emission, using a maximum likelihood approach to optimize the values of the model parameters and estimate the covariance matrix. The link between the model and data is provided by the instrument response functions describing the point-spread function, effective area, and energy dispersion of the LAT. However, uncertainties in these functions, and certain approximations made in applying them to the LAT data, will produce systematic errors in the parameters of fitted spectra. For bright gamma-ray emitters on long timescales, these systematic effects may be larger than the statistical errors. We present methods for evaluating the size of the systematic errors which arise from uncertainties in the effective area curve.

1. The bracketing-IRF method:

In this method, modified sets of instrument response functions (IRFs) are used to evaluate the effects of uncertainties in the effective area curve on the fitted spectral parameters. The procedure is as follows: (1) Evaluate the parameters of the spectral model in the normal way, using the standard LAT data analysis tools, *ScienceTools*, and the standard IRFs, for example *P6_V11_DIFFUSE*. (2) Produce sets of modified IRFs designed to affect each of the model parameters maximally within the estimated uncertainty on the effective area curve. (3) Rerun the analysis with each set of modified IRFs and note the changes in the spectral parameters of the source of interest, which give the systematic errors. In this poster we present sets of bracketing IRFs appropriate to evaluating the systematic errors on the flux and spectral index of a power-law fit.

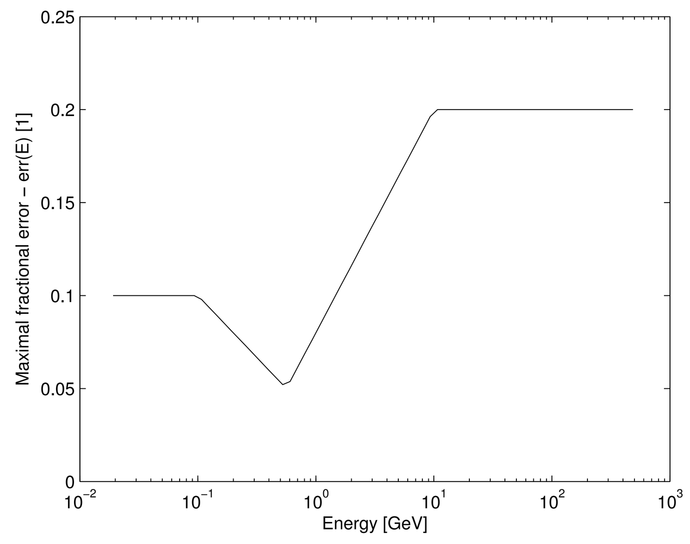

Fig. 1: Fractional error function, *err(E)*, with values of 10% at 100MeV, 5% at 575MeV and 20% at 10GeV.

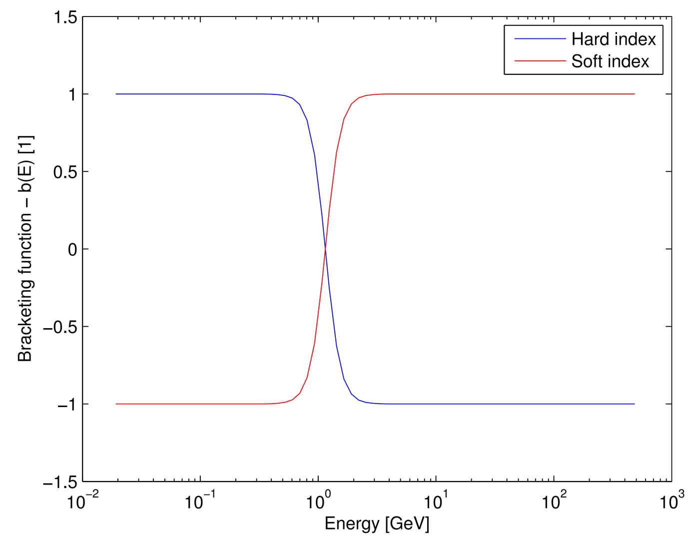

Fig. 2: Smoothed-step bracketing error function, *b(E)*, for evaluating systematic error on power-law index.

For each set of modified IRFs the effective area curve is scaled using the maximum absolute fractional error function, *err(E)*, as shown in Figure 1, modulated by a *bracketing function*, *b(E)*, chosen to affect the parameter of interest. The modified effective area is produced from the nominal value according to:

$$A_{mod}(E) = A_{nom}(E) \times (1 + b(E) \times err(E)). \qquad \text{(Eq. 1)}$$

For a power-law model two sets of bracketing functions are used. The first set consists of constant-valued functions, $b(E)=\pm 1$, which are used to evaluate the systematic errors on the flux constant of the power law. The second set consists of smoothed step functions, defined by $b(E)=\pm\tanh(\log_{10}(E/E_{pivot})/K)$, centered on the pivot energy of the nominal power-law fit, E_{pivot}, with smoothing factor of $K=0.13$, which are used to evaluate the systematic error on the spectral index of the power law. An example of the second set of functions is shown in Figure 2, centered on an energy of 1.15GeV, the pivot energy derived from an analysis of 1-year of Fermi-LAT data from the TeV blazar Mrk 421, using the standard P6_V11_DIFFUSE IRFs. The modified effective area curves produced with these bracketing functions are shown in Figure 3.

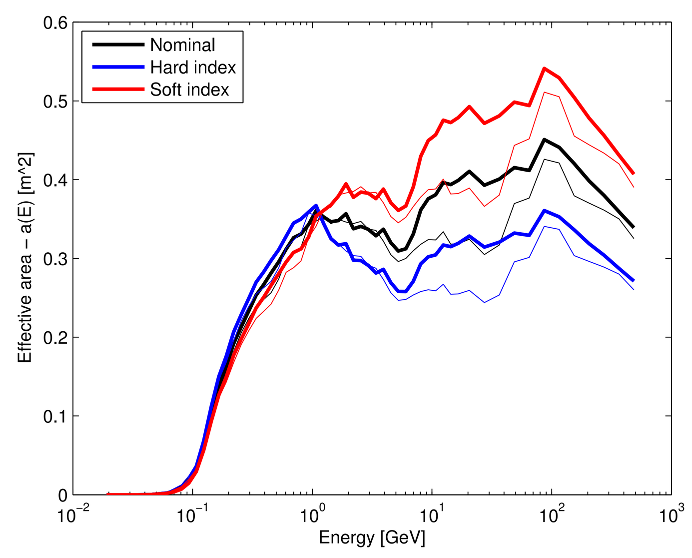

Fig. 3: Modified effective areas for P6_V11_DIFFUSE IRFs, front-converting (thick curves) and back-converting events (thin curves).

Table 1: Results of power-law fits to sample dataset using bracketing IRFs.

IRF set	Integral flux [10^{-8} ph/cm²/s]	Photon Index
Nominal, P6_V11_DIFFUSE	168.3 ± 5.6	1.771 ± 0.019
Flux high, constant b(E)=-1	178.3 ± 5.8	1.731 ± 0.019
Flux low, constant b(E)=+1	159.2 ± 5.3	1.801 ± 0.018
Index soft, b(E) as in Fig. 2	**157.3 ± 5.0**	**1.847 ± 0.019**
Index hard, b(E) as in Fig. 2	**182.1 ± 6.2**	**1.688 ± 0.019**

The results of power-law fits to the 1-year Mrk 421 dataset are shown in Table 1. In this example the nominal value of and statistical error on the spectral index is $\Gamma=1.771\pm0.019$. The systematic errors derived with this method are $\Delta\Gamma_{syst}=+0.076/-0.103$, considerably larger than the statistical error for this bright source. It should also be noted that, due to the correlation between the integral flux and spectral index, the largest change in the integral flux is seen in the results derived with the IRFs used to study the spectral index, and these values should be quoted. Again, the systematic errors of $\Delta F_{syst}=+13.8/-11.0 \times 10^{-8}$ph/cm²/s are larger than the statistical errors, showing the importance of studying the systematic errors for bright sources.

2. The Monte Carlo and bootstrap method:

A Bayesian approach would marginalize over the distribution of plausible effective area curves, *p(A)*, to obtain the posterior distribution of the fit parameters *θ*, given the data *D*:

$$p(\theta) = \int p(A)p(\theta|D,A)dA.$$

Here $p(\theta|D,A)$ is the likelihood used to fit the data. This integral would be evaluated over some multi-dimensional space that spans possible $A(E)$s, either parametrically or as tabulations of families of curves. In general, it is too computationally expensive to evaluate $p(\theta)$ by direct integration. Monte Carlo methods are often used instead: For each trial *k*, draw an effective area curve from its pdf, $A_k \sim p(A)$. Given that curve, compute the likelihood and draw the model parameters using that likelihood as the posterior pdf, i.e., $\theta_k \sim p(\theta|D,A_k)$. The resulting θ_ks would then provide an estimate of the posterior distribution of the model parameters. Since evaluating $p(\theta|D,A_k)$ over the θ-parameter space is itself computationally difficult, Lee et al. (2011) have proposed a Markov Chain Monte Carlo approach that would only require evaluating $p(\theta|D,A_k)$ at specific trial points of θ_k.

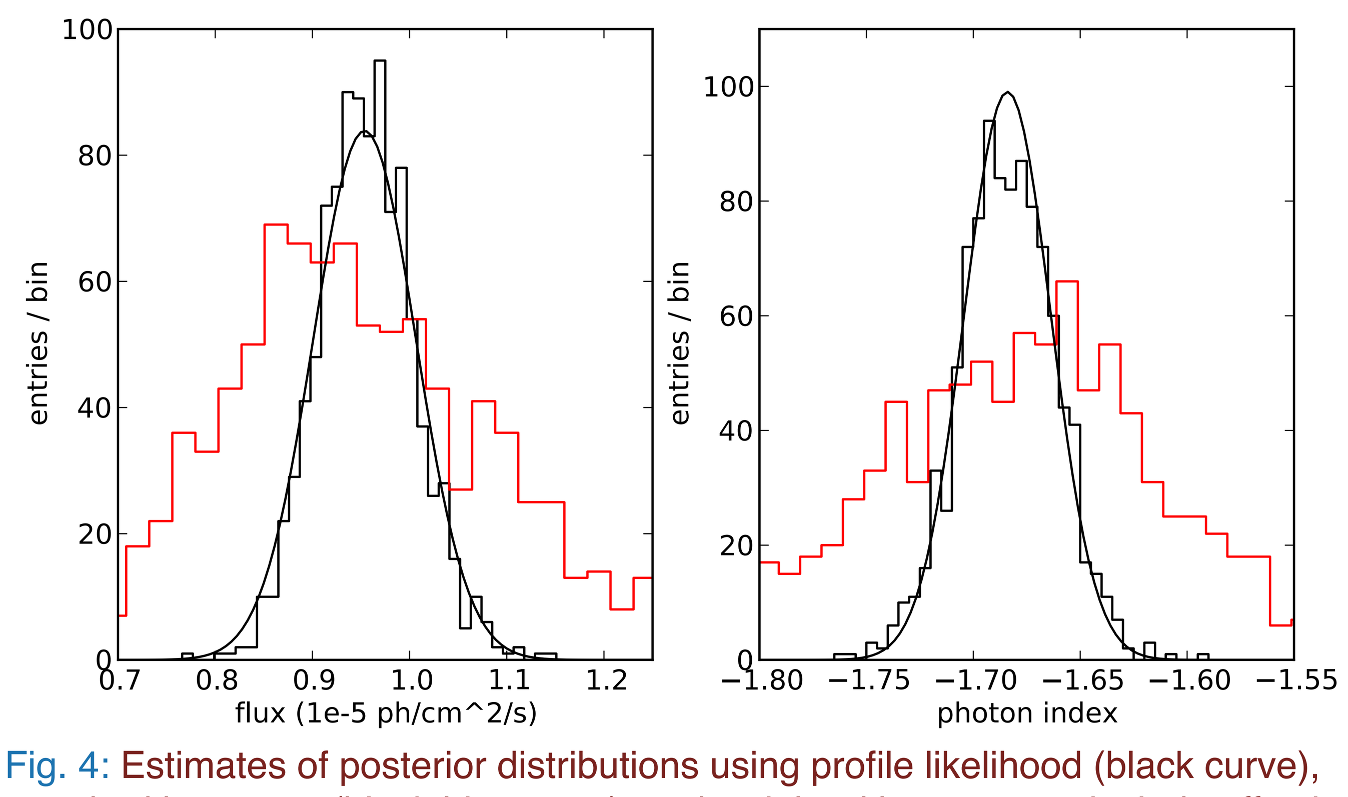

Fig. 4: Estimates of posterior distributions using profile likelihood (black curve), standard bootstrap (black histogram), and weighted bootstrap to include effective area systematic uncertainties (red histogram).

All of these approaches, including the bracketing method, involve recomputing the likelihood under the assumption of alternative effective area curves. For LAT data, because the A_ks must be integrated over a constantly changing observing profile, these methods can still impose a large computational burden. Instead of re-evaluating the likelihood of the observed data using alternative effective areas, we consider alternative datasets that are generated under the different A_ks and evaluate the likelihood using the nominal IRFs. This can be accomplished via a weighted bootstrap resampling of the event data. In standard bootstrap methods, simulated datasets are drawn via direct resampling (with replacement) of the observed data. To mimic the effect of generating data under an alternative A_k, we define a probability factor for each candidate event *i*:

$$P_{ik} = A_k(E_i,\theta_i,\phi_i)/A_{nom}(E_i,\theta_i,\phi_i),$$

where E_i, θ_i, and ϕ_i are the photon energy and aspect angles in instrument coordinates (This prescription neglects that these are measured quantities, whereas *A* is defined in terms of true quantities). For $P_{ik} \le 1$, event *i* is retained in the sample if $\xi < P_{ik}$, where ξ is a random uniform deviate on $[0,1)$. If $P_{ik} > 1$, then event *i* is retained and a copy of *i* is also added if $\xi < P_{ik} - 1$ (This is assumes $P_{ik} \le 2$, but it can be easily generalized). In standard bootstrap, $P_{ik} \equiv 1$.

Table 2: Fit parameters and errors from the various posterior estimators.

Estimator	Integral flux [10^{-5} ph/cm²/s]	Photon Index
Profile likelihood	0.954 ± 0.053	1.684 ± 0.020
Standard bootstrap	0.954 ± 0.049	1.684 ± 0.022
Weighted bootstrap	0.968 ± 0.164	1.684 ± 0.072

As an example of these methods, we show in Fig. 4, distributions of integral flux and photon index for a simulated point source using straight bootstrap (black histograms) with the profile likelihood distributions overlaid (black curves). We also plot the distributions obtained using the weighted bootstrap (red histograms). For those, we apply a modification of Eq. 1 to generate the family of effective area curves,

$$A_k(E) = A_{nom}(E) \times (1 + n_k \times |b(E)| \times err(E)),$$

where $n_k \sim \mathcal{N}(0,1)$, i.e., drawn from a normal distribution with zero mean and unity variance.

References: Lee, et al., arXiv:1102.4610 (2011)